

Plasma sheet structure in the magnetotail: kinetic simulation and comparison with satellite observations

Paolo Ricci^(1,2), Giovanni Lapenta^(1,3) and J. U. Brackbill⁽⁴⁾

(1) Istituto Nazionale per la Fisica della Materia (INFM), Dipartimento di Fisica, Politecnico di Torino, Torino, Italy

(2) Dipartimento di Energetica, Politecnico di Torino, Torino, Italy

(3) Theoretical Division, Los Alamos National Laboratory, Los Alamos NM USA

(4) Department of Mathematics and Statistics, University of New Mexico, Albuquerque NM

P. Ricci, Dipartimento di Energetica, Politecnico di Torino, Corso Duca degli Abruzzi 24 - 10129 Torino, Italy.

G. Lapenta, Los Alamos National Laboratory, Los Alamos NM 85744 (lapenta@lanl.gov).

J.U. Brackbill, Department of Mathematics and Statistics, University of New Mexico, Albuquerque NM.

Abstract.

We use the results of a three-dimensional kinetic simulation of an Harris current sheet to propose an explanation and to reproduce the ISEE-1/2, Geotail, and Cluster observations of the magnetotail current sheet structure. Current sheet flapping, current density bifurcation, and reconnection are explained as the results of the kink and tearing instabilities, which dominate the current sheet evolution.

1. Introduction

The magnetotail current sheet is one of the key topics in magnetospheric physics. A useful but simple one-dimensional description of the current sheet is given by the Harris model, where the magnetic field is given by $B_x(z) = B_0 \tanh(z/\lambda)$ and the plasma density, proportional to the current density, is given by $n(z) = n_0 \cosh^{-2}(z/\lambda)$, where λ is the half thickness of the current sheet and the GSM coordinates are used.

Observations of the current sheet have revealed a more complex structure. At the end of April 2, 1978, the ISEE-1/2 spacecraft detected a flapping of the plasma sheet and the spacecraft crossed the central region more than 10 times in a hour. In particular, during a "turbulent" crossing, the spacecraft detected current concentration outside the central region, unlike the Harris current sheet [Sergeev *et al.*, 1993]. In fact, Geotail [Kokobun *et al.*, 1994; Mukai *et al.*, 1994] averaged data obtained from October 1993 to June 1995 show that the the structure of the plasma sheet can be often approximated by a double-peaked electric current sheet [Hoshino *et al.*, 1996] and observations made by the same spacecraft during a substorm on 23 April 1996 substorm lead to similar conclusion [Asano *et al.*, 2003]. On January 14, 1994, Geotail also detected multiple double-peaked current sheet crossings, associated with plasma flow [Hoshino *et al.*, 1996]. More recently, time analysis of data from the four Cluster spacecrafts [Balogh *et al.*, 2001] showed that fast motion and bifurcation of the current sheet are associated with a wave-like transient propagating in the dawn-to-dusk direction [Sergeev *et al.*, 2003; Runov *et al.*, 2003]. These observations refer both to the distant magnetotail ($\approx 100R_E$) [Hoshino *et al.*, 1996] and to a region closer to Earth ($\approx 15R_E$) [Sergeev *et al.*, 1993; Asano *et al.*, 2003; Runov *et al.*, 2003; Sergeev *et al.*, 2003]

Generalizations of the current sheet equilibria have been recently proposed to reproduce the features observed by satellites [*Shindler and Birn, 2002; Sitnov et al., 2003*]. Runov *et al.* [2003] propose that these signatures are due to a kink or a sausage instability of a current sheet with an enhanced current density on both hemispheres. Zelenyi *et al.* [2002] show that non-adiabatic effects can reduce the current density in the center of the current sheet. A bifurcated current sheet can be present in the plasma outflow region when magnetic reconnection is occurring [e.g., *Arzner and Sholer, 2001*]. Karimabadi *et al.* [2003a, 2003b] argue that the ion-ion kink instability causes a displacement of the current sheet which can explain the observations. They show that the observed flapping wavelength quantitatively agrees with the linear theory of the ion-ion kink instability. Their hybrid and kinetic simulations confirm the evolution of the kink mode and explain the bifurcated structure of the current sheet as a magnetic field profile with weak central gradient.

In the present work, we use the results of a three-dimensional kinetic simulation of the Harris current sheet to show that a kink instability and the self-consistent evolution of the current, including reconnection, can be responsible for the data described in the references above. In particular, taking into account the relative motion of the current sheet and the spacecraft, and the Cluster tetrahedron configuration, we recover the most significant magnetic data records obtained by the Cluster spacecraft. The data can be interpreted as the signature of current sheet flapping and bifurcation. The magnetic field B_x and the current density J_y are spatially averaged to allow comparison with results by Hoshino *et al.* [1996]. We also compare the plasma flow due to the tearing instability with the observations [*Hoshino et al., 1996; Øieroset et al., 2001; Asano et al., 2003*].

2. Three-dimensional simulations

In our study, we use the implicit PIC code CELESTE3D [*Forslund and Brackbill*, 1985; *Vu and Brackbill*, 1992; *Ricci et al.*, 2002a], which is particularly suitable for large scale and long period kinetic simulations performed with high mass ratio and has been applied previously to problems in magnetospheric physics [e.g., *Lapenta and Brackbill*, 2000; *Lapenta and Brackbill*, 2002; *Ricci et al.*, 2002b; *Lapenta et al.*, 2003]. We use the same plasma parameters as the GEM challenge [*Birn et al.*, 2001], in particular $\lambda = 0.5c/\omega_{pi}$, $T_i/T_e = 5$, the ion drift velocity is $V_{i0} = 1.67V_A$, and we add a background population, so that $n(z) = n_0 \cosh^{-2}(z/\lambda) + n_b$, with $n_b = 0.2n_0$. Unlike the GEM challenge, we do not add any initial perturbation and let the system evolve on its own. The dimensions of the system are $[-L_x/2, L_x/2] \times [-L_y/2, L_y/2] \times [-L_z/2, L_z/2]$ with $L_x = 12.8c/\omega_{pi}$, $L_y = 19.2c/\omega_{pi}$, and $L_z = 6.4c/\omega_{pi}$. The mass ratio is $m_i/m_e = 180$. The parameters chosen make the current sheet particularly unstable and its dynamics are accelerated compared with typical magnetotail current sheets. We are constrained to do that in order to follow the dynamics of the current sheet in a reasonable computational time. As a consequence, it is necessary to scale our results to make a quantitative comparison between simulation results and observations. In any case, the general trends can be located and the linear theory [*Karimabadi et al.*, 2003a] can help in scaling the results.

Previous simulations [*Lapenta and Brackbill*, 2002; *Lapenta et al.*, 2003; *Daughton*, 2003] performed in the current aligned plane show, in absence of a plasma background, the development of the fastest lower-hybrid drift instability on the electron gyroscale, followed by electromagnetic modes with wavelengths intermediate between the ion and the electron gyroscale. The lower hybrid drift instability causes a velocity shear (present since

the beginning of the simulation when a background plasma is present) that triggers a Kelvin-Helmhotz instability that kinks the current sheet. Three-dimensional simulations have shown that the kinking of the current sheet triggers a tearing instability [*Lapenta and Brackbill, 2001; Lapenta et al., 2003*]. As we add a background population, following Karimabadi *et al.* [2003b], the velocity shear is present since the beginning of the simulation and the resulting Kelvin-Helmhotz instability can be also interpreted as a kinetic ion-ion kink instability [*Karimabadi et al., 2003a; Karimabadi et al., 2003b*].

Figure 1 shows fully developed current sheet kinking. The B_x field and the current density J_y are shown. The wavelength is $k_y\lambda \approx 0.5$, which matches fairly well the observed wavelength in Runov *et al.* [2003] ($k_y\lambda = 0.7$) . The linear theory, predicts a decrease of the wavelength when ρ_i/λ increases [*Karimabadi et al., 2003a*]. The amplitude A at time $t\omega_{ci} = 16$ is $A/\lambda \approx 2$ is comparable to the observed value ($A/\lambda \approx 1.4$) [*Sergeev et al., 2003*]. The flapping motion observed by Cluster moving duskward at $v_{ph} \approx 200$ km/s, corresponding to approximatively $0.2v_A$. The kink instability shown in our simulations gives a $v_{ph,SIM} \approx 0.5v_A$, larger than observed in space. However, the linear theory predicts a decrease of the phase velocity when ρ_i/λ increases. Since, we use an artificially high ρ_i/λ , the higher phase speed is justified and consistent with our interpretation of the flapping motion.

Below we consider specific aspects of the satellite observations basing their interpretation on the simulation.

3. Current sheet flapping

When vertical oscillations of the plasma sheet (flapping) occur, spacecrafts may repeatedly cross the current sheet. Clear evidence of current sheet flapping is shown by ISEE-1/2

[*Sergeev et al.*, 1996], by Geotail [*Hoshino et al.*, 1996], and by Cluster [*Runov et al.*, 2003; *Sergeev et al.*, 2003]. We focus our attention on the observations by Cluster and show that current sheet kinking developed in the course of our simulations can explain those.

In Fig. 2a we show Cluster #2 and #3 observations taken on 29 August 2001, which have been analyzed previously by *Runov et al.* [2003]. In particular, the B_x data is considered. In Fig. 3a, we evaluate the magnetic field as a function of time as would be recorded by a virtual spacecraft placed in the environment provided by the simulation. According to the real spacecraft disposition, we impose a distance between the two virtual satellites in the z direction to be of the order of $\lambda/2$. Cluster observes an oscillation period of $\tau = 90$ s and a relative velocity between satellite and plasma $v_{ph} \approx 0.2v_A$. In order to decrease the time necessary for the observation, we increase the relative satellite velocity up to $v_{SIM} = 5v_A$, thus decreasing the oscillation period to $\tau_{SIM} = 2\omega_{ci}^{-1}$, in good agreement with the oscillation period recorded by Cluster. With the new relative velocity and using the fact that $\omega_{ci} \approx 0.6s^{-1}$ in the magnetotail and the observed period is of the order $54\omega_{ci}^{-1}$, the observed wavelength, $v_{ph}\tau \approx 11c/\omega_{pi}$ and the simulated wavelength, $v_{SIM}\tau_{SIM} \approx 10c/\omega_{pi}$, are comparable.

The flapping observation recorded by Cluster #3 on September 26, 2001 and described by *Sergeev et al.* [2003] is shown in Fig. 2b. It is reproduced by our simulations at later times, when the amplitude of the kink has grown enough that the virtual satellite can pass from one side to the other of the current sheet. This is shown in Fig. 3b. We note that Cluster observations reveal a flattening of the current sheet in the vicinity of the points where $B_x = 0$. This may be the result of higher frequency kink modes, which have been shown in more detailed explicit two-dimensional simulations [*Daugthon*, 2003].

In agreement with Sergeev *et al.* [2003] and Runov *et al.* [2003], our simulations reveal that the current sheet flapping is mostly in the (y, z) plane, while the tilt in the (x, z) plane is insignificant.

4. Current sheet bifurcation

Experimental evidence exists that the current distribution in the magnetotail sheet may be double-peaked, with a pair of electric current sheets separated by a layer of a weak quasi-uniform magnetic field. Current sheet bifurcation has been revealed both in single sheet crossings, and in averages over a number of current sheet crossings. For example, Runov *et al.* [2003] compare the observations of two Cluster satellites and show that $\partial B_x / \partial z \approx 0$ when $B_x \approx 0$. (This is unlike the Harris sheet equilibrium, where $\partial B_x / \partial z$ is maximum at $z = 0$ where $B_x = 0$.) Statistical studies of the current sheet are presented in Hoshino *et al.* [1996], revealing a bifurcated current profile. The bifurcated current profile is also reflected in the distribution of the values of the B_x field, as the number of observations of small guide fields is greater than what expected in the case of a Harris sheet equilibrium [Hoshino *et al.*, 1996; Sergeev *et al.*, 2003], and in the change of the $\partial B_x / \partial z$ profile, as a function of B_x as the peak is shifted from the center of the current sheet to the region where $B_x \approx 0.5B_0$.

Figure 1 shows that the kink instability produces a self-consistent change in the current density. This change can explain the satellite observations, both single crossing and averaged signatures.

A single crossing signature is shown in Fig. 2c from 29 August 2001 observations of Cluster #3 and #4 considered by Runov *et al.* [2003]. Conversely to the case of standard Harris sheet, near the point where $B_x \approx 0$ the magnetic fields measured by the two

satellites are equal, even though the distance between the satellites is of the order of the current sheet thickness. This indicates that the current profile is not peaked at the center of the sheet. In Fig. 3c, we show that similar observations are found within our simulation. The distance between the two virtual satellites is also of the order of λ .

An average over x and y of the current density J_y and the $\partial B_x / \partial z$ profiles are shown in Fig. 4 at $t = 0$ and $t\omega_{ci} = 20$. Assuming that the spatially averaged current profiles can be compared with the averaged observations of many current sheet crossings, we show that the profiles at $t\omega_{ci} = 20$ agree remarkably with the results of the Geotail observations which have been averaged by Hoshino *et al.* [1996]. The current is depleted at the center of the current sheet and two current peaks grow on the flanks of the initial current sheet. Furthermore, $\partial B_x / \partial z$ is no longer peaked at the center of the current sheet. Instead, it is rather flat (this kind of measure is generally very noisy) and slightly peaked at $B_x \approx 0.5$.

We finally remark that observations by Geotail on 23 April 1996 show that positive $d|B_x|/dt$ corresponds to relevant current density J_y [Asano *et al.*, 2003]; the same effect is also recovered within our simulation.

5. Reconnection

Not only does a kink instability grow, but also a tearing instability develops in the Harris sheet, which leads to the reconnection of the magnetic field lines and outflow and inflow plasma jets. Satellite observations typically reveal the reconnection process either by detecting inflow and outflow plasma jets, which can be very noisy [e.g., Asano *et al.*, 2003], or by detecting earthward and tailward plasma jets with velocities of the order of $0.1v_A$ or bigger [Hoshino *et al.*, 1996], or even by detecting flow reversal [Øieroset *et al.*, 2001]. In Fig. 5 we show signatures of magnetic reconnection by showing a flow

reversal associated with a change in the sign of the reconnecting field. The earthward and tailward velocities, detected during the crossing of the current sheet, are of the order of $0.1v_A$, which roughly corresponds to the typical order of magnitude of plasma velocity in the satellite observations.

6. Conclusion

We remark that the kink instability developed here is due to the velocity shear caused by the presence of a background population, as shown by Karimabadi *et al.* [2003a, 2003b]. If there is no background density, the kink can grow because of the nonlinear development of the Lower Hybrid Drift Instability that modifies the velocity profile and causes a shear in the velocity [Lapenta and Brackbill, 2002].

We have chosen to start from a relatively thin and unstable current sheet ($\lambda/d_i = 0.5$). Such thin current sheets are indeed observed in the magnetotail [e.g., Asano *et al.*, 2003, for a review]. It is possible that for thicker current sheets the tearing instability is stabilized by the presence of a B_z field, while the kinking is unstable.

Acknowledgments. The authors gratefully thank M. Hoshino for the permission to use the data plotted in Fig. 4 and J. Birn, J. Chen, W. Daughton, I. Furno, M. Taylor, A. Vaivads for helpful discussions. The satellite data has been obtained from Cluster FGM team [Balogh *et al.*, 2001]. This research is supported by the Laboratory Directed Research and Development (LDRD) program at the Los Alamos National Laboratory, by the United States Department of Energy, under Contract No. W-7405-ENG-36 and by NASA, under the "Sun Earth Connection Theory Program". The supercomputer used

in this investigation was provided by funding from JPL Institutional Computing and Information Services and the NASA Offices of Space Science and Earth Science.

References

Arzner, K., and M. Sholer, Kinetic structure of the post plasmoid plasma sheet during magnetic reconnection, *J. Geophys. Res.*, 106, 3827, 2001.

Asano, Y., et al., Evolution of the thin current sheet in a substorm observed by Geotail, *J. Geophys. Res.*, 108(A5), 1189, doi: 10.1029/2002JA009785, 2003.

Balogh, A., et al., The Cluster magnetic field investigation: Overview of in-flight performance and initial results, *Ann. Geophys.*, 19, 1207, 2001.

Birn, J. et al., Geospace Environment Modelling (GEM) magnetic reconnection challenge, *J. Geophys. Res.*, 106, 3715, 2001.

Brackbill, J. U. and D. W. Forslund, Simulation of low frequency, electromagnetic phenomena in plasmas, in *Multiple times Scales*, J.U. Brackbill and B.I. Cohen Eds., (Academic Press, Orlando, 1985), pp. 271-310.

Daughton, W.S., Electromagnetic properties of the lower-hybrid drift instability in a thin current sheet, *Phys. Plasmas*, submitted, 2003.

Hoshino, M., et al., Structure of plasma sheet in magnetotail: Double-peaked electric current sheet, *J. Geophys. Res.*, 101, 24775, 1996.

Lapenta, G., and J.U. Brackbill, 3D reconnection due to oblique modes: a simulation of Harris current sheets, *Nonlinear Processes Geophys.*, 7, 151, 2000.

Lapenta, G., and J.U. Brackbill, Nonlinear evolution of the lower hybrid drift instability: Current sheet thinning and kinking, *Phys. Plasmas*, 9, 1544, 2002.

Lapenta, G., J.U. Brackbill, and W.S. Daughton, The unexpected role of the lower hybrid drift instability in magnetic reconnection in three dimensions, *Phys. Plasmas*, **10**, 1577, 2003.

Karimabadi, H., P.L. Pritchett, W. Daughton, and D. Krauss-Varban, Ion-ion kink instability in the magnetotail 1. Lineary Theory, *J. Geophys. Res.*, in press (2003a).

Karimabadi, H., P.L. Pritchett, W. Daughton, and D. Krauss-Varban, Ion-ion kink instability in the magnetotail: 2. Three-dimensional full particle and hybrid simulations and comparison with observations, *J. Geophys. Res.*, in press (2003b).

Kokobun, S., et al., The GEOTAIL magnetic field experiment, *J. Geomagn. Geoelectr.*, **46**, 4, 1994.

Mukai, T.S., et al., The low energy particle (LEP)experiment on board the GEOTAIL satellite, *J. Geomagn. Geoelectr.*, **46**, 669, 1994.

Øieroset, M, T.D. Phan, M. Fujimoto, R.P. Lin, R.P. Lepping, In situ detection of collisionless reconnection in the Earth's magnetotail, *Nature*, **412**, 414, 2001.

Ricci, P., G. Lapenta, and J.U. Brackbill, A simplified implicit Maxwell solver, *J. Comput. Phys.*, **183**, 117, 2002a.

Ricci, P., G. Lapenta, and J.U. Brackbill, GEM reconnection challenge: Implicit kinetic simulations with the physical mass ratio, *Geophys. Res. Lett.*, **29**(23), 2088, doi:10.1029/2002GL015314, 2002b.

Runov, A., et al, Cluster observation of a bifurcated current sheet, *Geophys. Res. Lett.*, **30**(2), 1036, doi:10.1029/2002GL016136, 2003.

Sergeev, V.A., D.G. Mitchell, C.T. Russel, and D.J. Williams, Structure of the Tail Plasma/Current sheet at $\approx 11 R_E$ and its changes in the course of a substorm, *J.*

Geophys. Res., 98, 17345, 1993.

Sergeev, V., et al., Current sheet flapping motion and structure observed by Cluster,

Geophys. Res. Lett., 30(6), 1327, doi: 10.1029/2002GL016500, 2003.

Shindler, K., and J. Birn, Models of two-dimensional embedded thin current sheets from

Vlasov theory, *J. Geophys. Res.*, 107(A8), doi: 10.1029/2001JA000304, 2002.

Sitnov, M.I., P.N. Guzdar, and M. Swisdak, A model of the bifurcated current sheet,

Geophys. Res. Lett., 30(13), 1712, doi: 10.1029/2003GL017218, 2003.

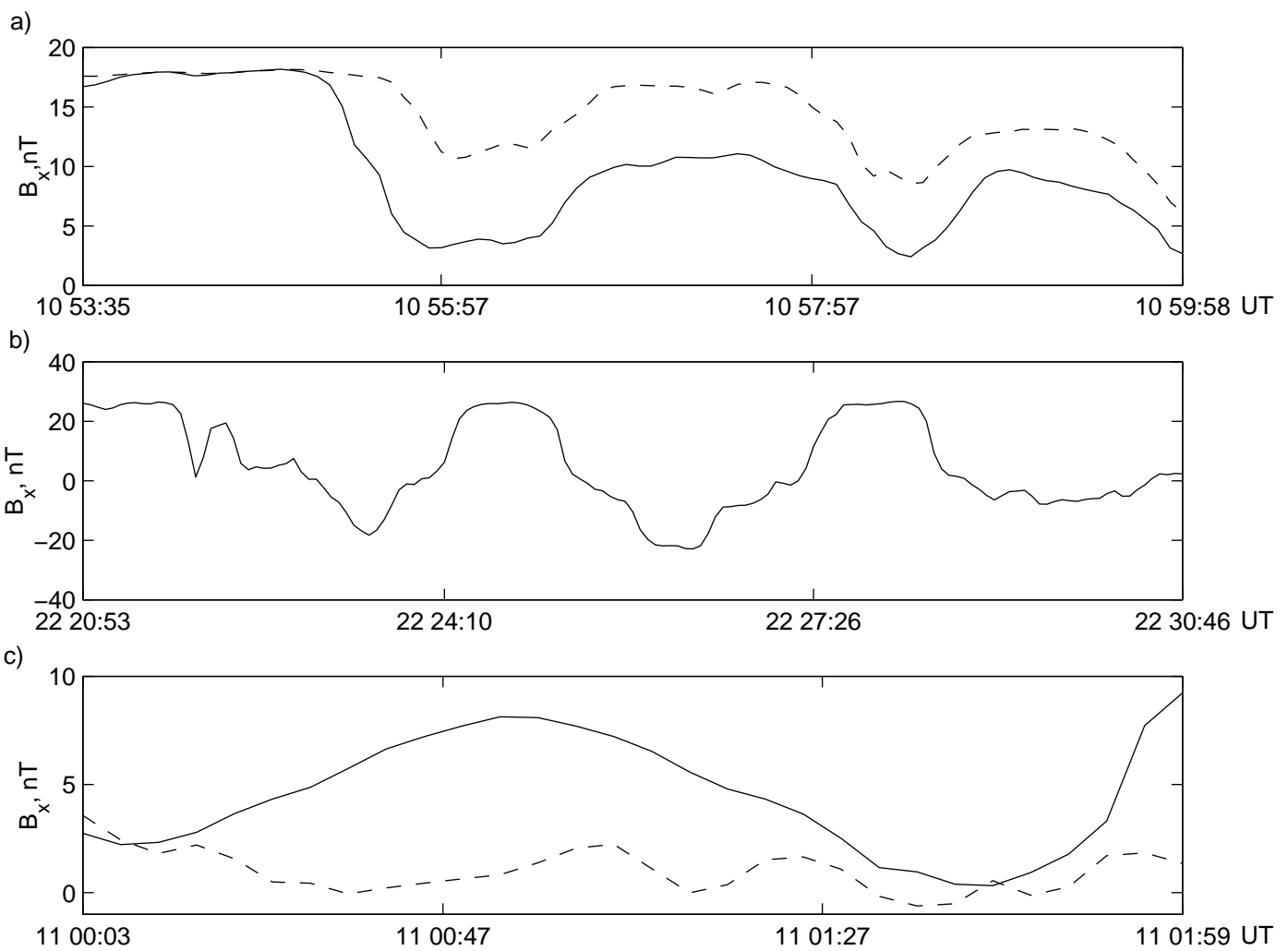
Vu, H. X. and J. U. Brackbill, CELEST1D: An implicit, fully kinetic model for low-

frequency Electromagnetic plasma simulation, *Comput. Phys. Commun.*, 69, 253, 1992.

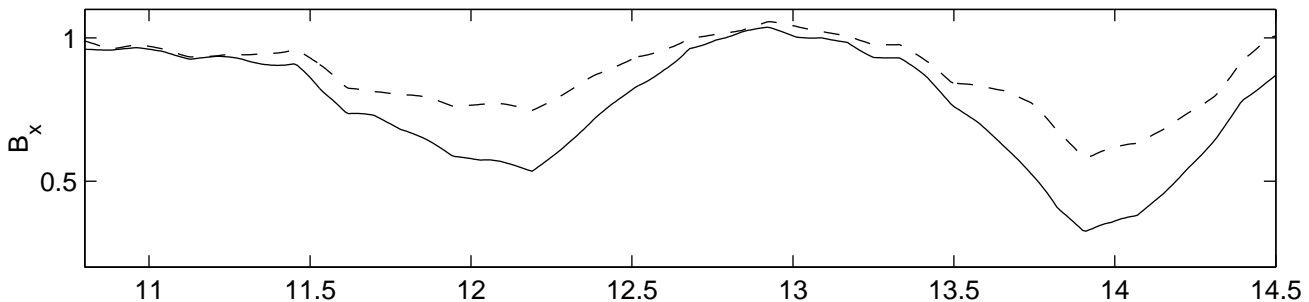
Zelenyi, L.M., D.C. Delcourt, H.V. Malova, and A.S. Sharma, "Aging" of the Magnetotail

thin current sheet, *Geophys. Res. Lett.*, 29(12), doi:10.1029/2001GL013789, 2002.

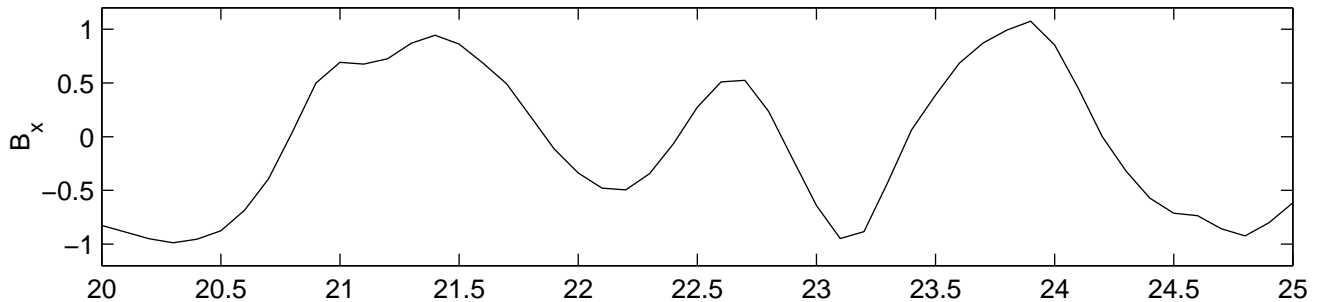
- Fig. 1: The kink of the current sheet is presented by showing (a) the x component of magnetic field, B_x , and (b) the y component of the current density, J_y . Both quantities are shown as a function of y and z , at time $t\omega_{ci} = 16$ and at $x = 0$. B_x is normalized to B_0 , J_y to en_0V_A .
- Fig. 2: Signatures of current sheet flapping (a,b) and weak current density at the center of the current sheet (c), observed by the FGM Cluster experiment [Balogh *et al.*, 2003]. We report the B_x magnetic field recorded by satellites #2 (dashed) and #3 (solid) on 29 August 2001 that has been described by Runov *et al.* [2003] (a); by satellite #3 on September 26 2001, described by Sergeev *et al.* [2003]; by satellites #3 (dashed) and #4 (solid) on 29 August 2001, described by Runov *et al.* [2003] (c).
- Fig. 3: Signatures of current sheet flapping (a,b) and weak current density at the center of the current sheet (c) as would be recorded by a virtual spacecraft placed in the environment provided by the simulation and which reproduce the real signature shown in Fig. 2. The B_x magnetic field is plotted, normalized to B_0 .
- Fig. 4: Current density profile (a) and gradient of the current sheet (b) averaged over x and y , at time $t = 0$ (dashed, unperturbed Harris current sheet) and at time $t\omega_{ci} = 20$ (solid). The tick solid line represents the Geotail averaged observations [Hoshino *et al.*, 2003, Fig. 4b], where the original dimensionless units have been scaled to fit the simulation results.
- Fig. 5: Typical signature of reconnection: during the crossing of the current sheet [the satellite trajectory shown in the (x, z) (a) and in the (x, y) plane (b)] the reconnecting field, B_z , changes sign (c) and it is associated to earthward and inward plasma jets (d).



a)



b)



c)

